Ninth International Conference on
THIN-WALLED STRUCTURES – ICTWS2023
Sydney, Australia, Nov 29 – Dec 1, 2023

# MOMENT CAPACITY OF BRACKETS OF COLD-FORMED STEEL PORTAL FRAMES

**Xin Chen*, Megan Boston**, Krishanu Roy** and James B.P. Lim ****

* Department of Civil and Environmental Engineering, The University of Auckland, New Zealand
e-mail: xche889@aucklanduni.ac.nz

** School of Engineering, University of Waikato, New Zealand
e-mails: megan.boston@waikato.ac.nz, kris.roy@waikato.ac.nz, jlim@waikato.ac.nz

**Keywords**: Portal frames, Cold-formed steel, Moment capacity of brackets, Finite element analysis.

**Abstract**. *The strength and stiffness of cold-formed steel portal frames are heavily related to the performance of their joints; these joints are normally formed through brackets, bolted to the webs of channels. They should have adequate strength to ensure the frame fails within the members, and the design moment capacity of a joint should be equal to or exceed the moment to which the joint is subjected. Previous research in the literature, however, has not provided design equations for either the apex or eaves brackets, and any guidance found has been limited to closing or opening moment, joints fully restrained against lateral-torsional buckling, or joints composed of back-to-back brackets connecting back-to-back channels. This paper describes a finite element study comprising 10,080 models, that addresses all these limitations. Unified equations are presented that can be used for the design of both the apex and eaves brackets in practical partially restrained joints, as found in New Zealand practice, both closing and opening moments, both single and back-to-back brackets with the top-bottom stiffeners.*

## 1 INTRODUCTION

In New Zealand, cold-formed steel (CFS) channels are a popular choice for the primary load-carrying members of portal frames [1,2] (see Figure 1). In such moment-resisting structures, the apex, and eaves joints (see Figure 2) are commonly formed through bolting brackets to the webs of connecting members. This connection method creates semi-rigid joints [3].

Figure 1: Photograph of a CFS portal frame building.

The overall strength and stiffness of CFS portal frames are affected by the bracket detailing (i.e. overall dimensions and thickness of the bracket, number of fasteners, etc.) [4-6]. Guidance in AS/NZS4600: 2018 [4] is limited to stating that joints should be designed to have adequate strength and ductility to ensure the structure fails within the members, and no guidance is provided on the detailing of the joints.

(a) Apex joint (b) Eaves joint

Figure 2: Apex and eaves joint used in CFS portal frames.

Academic studies [7] provided guidance for sizing eaves brackets used in CFS portal frames, however, the proposed method was limited to fully restrained joint arrangements matching a specifically idealised finite element (FE) model. The photograph in Figure 2 shows the partially restrained apex and eaves joint, a common arrangement in New Zealand practice. No guidance in the design standards or literature is provided for the design of partially restrained joints used in practice.

Joints are generally constructed following one of two arrangements: one bracket fastened to a single channel (1B1C), or two brackets bolted to back-to-back channels (2B2C), as shown in Figure 3. While guidelines for predicting the moment capacity of fully restrained eaves brackets in a configuration with one bracket and back-to-back channels (1B2C) have been previously developed by Lim and Nethercot [7], these are not valid for practical partially restrained configurations. Furthermore, they are only valid for the closing moment.

(a) One bracket and one channel (1B1C) (b) Two brackets and two channels (2B2C)

Figure 3: Diagram showing joint arrangements (dotted lines represent brackets).

This paper thus fills an existing research gap by investigating the closing and opening moment capacities of partially restrained apex and eaves brackets. Unified design equations are proposed for designing brackets with top-bottom stiffener arrangements, as shown in Figure 4.

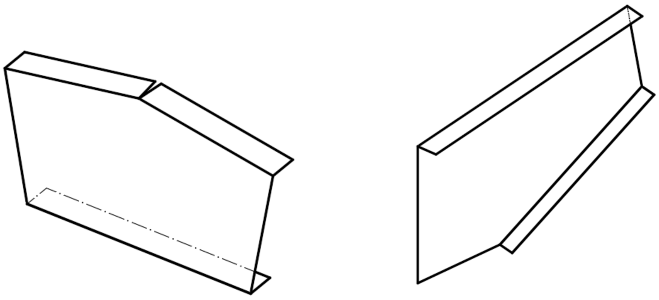

(a) Apex bracket (b) Eaves bracket

Figure 4: Brackets with top-bottom stiffeners.

## 2 THE EFFECT OF THE BRACKET ON THE CAPACITY OF THE CFS PORTAL FRAME

Lim and Nethercot [1] tested two portal frames (see Figure 5), to be referred to as Frames A and B. Chen et al. [8] validated the shell FE model of the portal frame against the experimental results, using the FE program ABAQUS [9]. The load-apex deflection curve comparison of the experimental and FEA results is shown in Figure 6. Overall, there is close agreement between the results of the experiment and the FE model. The FE model was validated against the full-scale portal frame test.

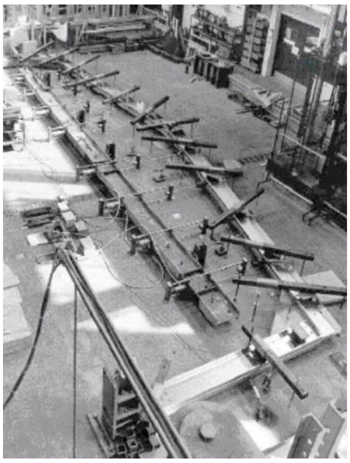

Figure 5: Full-scale portal frame test after Lim and Nethercot [1].

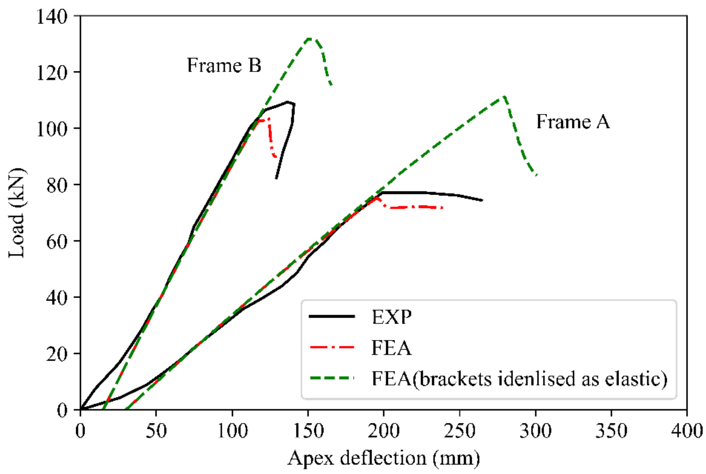


Figure 6: Load vs. apex deflection curve comparison of experimental and FEA results.

Both experimental and FEA results show that the portal frames failed due to the buckling of apex brackets (see Figure 7). To study the influence of joint brackets on the capacity of portal frames, the apex and eaves brackets were both set as linear elastic material in the FE model and the analyses were rerun. When brackets are idealised as elastic, the von Mises stress contour of the column is shown in Figure 8. The yielded area is shown as red colour and the failure mode is now buckling of the column near the eaves joint. Failure of the frame, in this case, occurs due to buckling of the CFS channel sections, influenced by the bi-moment as described by Lim et al. [10].

When failure occurs within the members, the load with the apex deflection curve is also shown in Figure 6, represented by the green dot lines. The ultimate load increased by 45% for

Frame A and 28% for Frame B. Furthermore, as the joint brackets influence the ultimate strength of the frame, it is necessary to accurately predict the capacity of brackets.

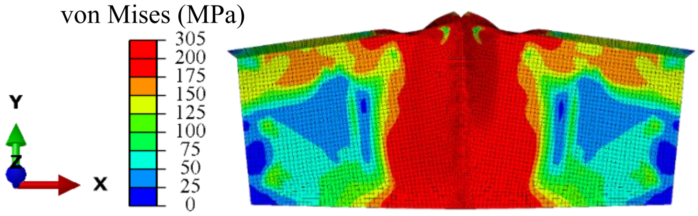


Figure 7: Stress contour of the apex bracket.

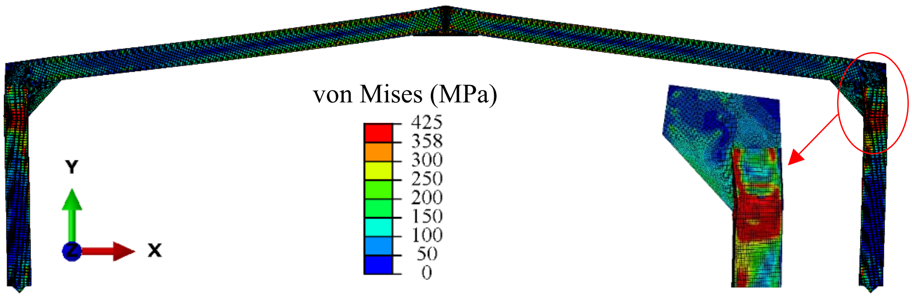


Figure 8: Stress contour of the right eave joint (brackets idealised as elastic).

## 3 MOMENT CAPACITY PREDICTION

### 3.1 Apex brackets with top-bottom stiffeners

A parametric study using the validated FE model [11] shown in Figure 9, for the partially restrained apex joint, is conducted to investigate the moment capacity of apex brackets. Six different cross-sectional geometries of the channels, designated by web size, are considered as summarised in the first column of Table 1. The channels are modelled as linear elastic to ensure failure in the brackets. The parameter of an apex bracket is shown in Figure 10.

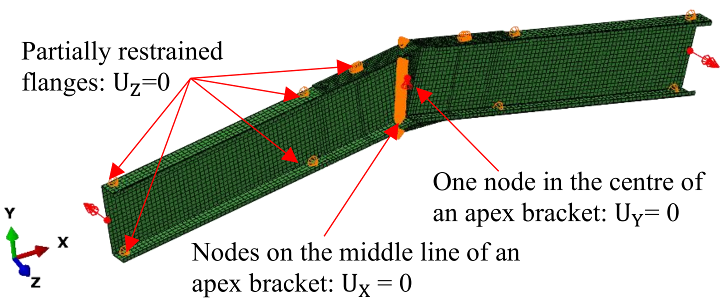


Figure 9: Partially restrained apex joint of 1B1C.

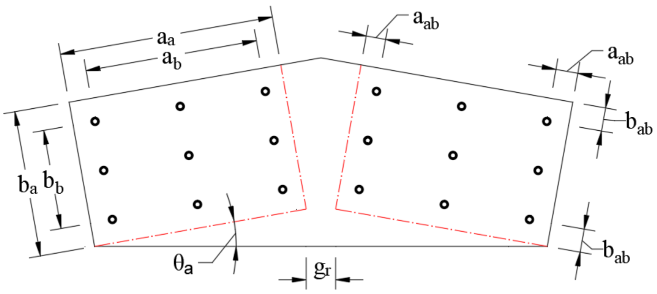


Figure 10: Diagram showing the parameter of an apex bracket (dotted lines represent the outlines of channels).

Table 1: Selected variable for parametric studies on apex joints.

| Channel | $b_a$ (mm) | $b_a/a_a$ | $t$ (mm) | $f_y$ (N/mm$^2$) | Unified geometric parametric |
|---|---|---|---|---|---|
| C150 | 150 | [0.4 ~ 0.9] | [2 ~ 4] | [250 ~ 550] | $\theta_a$ = 10°; $g_r$ = 10 mm; $a_{ab}$= $b_{ab}$ = 40 mm; $d_s = 1.95 a_a (t/a_a)^{0.543}$; Bolt distance ≤ 200 mm. |
| C200 | 200 | | | | |
| C250 | 250 | | | | |
| C300 | 300 | | | | |
| C350 | 350 | | | | |
| C400 | 400 | | | | |

### 3.1.1 Opening moment

The parametric study first analyses the opening moment for the apex joint of 1B1C using 1,260 FE models, from varying design parameters of an apex bracket. The remaining design parameters outlined in Table 1 are kept constant during the analysis to match the values normally seen in practice. Each of the varied design parameters covers values typically used in design following AS/NZS4600:2018 [4]. The edge width ($b_a$) is increased from 150 mm to 400 mm, and the ratio $b_a/a_a$ is varied between 0.4 and 0.9. Thickness varied from 2 mm to 4 mm in 0.5 mm increments. Seven different values of yield stress are assessed, starting at 250 $\mathrm{N/mm^2}$, increasing in 50 $\mathrm{N/mm^2}$ increments to 550 $\mathrm{N/mm^2}$.

In recent years, machine learning techniques have been employed to predict the strength of structural components [12]. Linear regression has been implemented using scikit-learn to fit a model with coefficients by minimizing the residual sum of squares between the observed data and the predicted data [13]. In this study, a linear regression algorithm is employed to develop a design equation for the moment capacity. The opening moment ($M_{o,tb}^{1a}$) of the single apex bracket can be calculated by the following equation:

$$M_{o,tb}^{1a} = 5.1645\, a_a^{0.5380}\, b_a^{0.8900}\, f_y^{0.5124}\, t^{1.6915}\, 10^{-5} \quad (1)$$

Where, units of $a_a$, $b_a$, and $t$ is mm, the unit of $f_y$ is $\mathrm{N/mm^2}$, and the unit of $M_{o,tb}^{1a}$ is kN.m.

The opening moment ($M_{o,tb}^{2a}$) of back-to-back apex brackets can be calculated by the following equation, based on the parametric study on 1,260 FE models, having double brackets connected with back-to-back channel sections (2B2C).

$$M_{o,tb}^{2a} = 5.3415\, a_a^{0.4652}\, b_a^{0.9519}\, f_y^{0.6412}\, t^{1.7447}\, 10^{-5} \quad (2)$$

### 3.1.2 Closing moment

Next, the moment capacity of the closing moment is analysed using the same parametric values as the previously discussed opening moment. These results in 2,520 FE models subjected to pure bending moment are assessed with variations, following the range of values given in Table 1.

As with the opening moment, the consistent trends provide means to create an empirical equation of the closing moment capacity of the apex bracket. This relationship between the closing moment capacity ($M_{c,tb}^{1a}$) of the single apex bracket is shown in the following equation.

$$M_{c,tb}^{1a} = 2.1323\, a_a^{0.4162}\, b_a^{1.1194}\, f_y^{0.6439}\, t^{1.4669}\, 10^{-5} \quad (3)$$

The closing moment ($M_{c,tb}^{2a}$) of back-to-back apex brackets can be calculated by the following equation:

$$M_{c,tb}^{2a} = 1.7463\ a_a^{0.4380}\ b_a^{1.0979}\ f_y^{0.7678}\ t^{1.6134}\ 10^{-5} \tag{4}$$

Some statistical expressions, such as the coefficient of determination ($R^2$), mean-absolute-percentage error (*MAPE*), root-mean-square deviation (*RMSE*), and the mean and standard deviation of the ratio of anticipated and actual values (*AVE* and *STD*) can be used to assess the accuracy of a prediction model [14]. Statistical results of the predicted moment capacities of apex brackets are tabulated in Table 2. This outcome demonstrates that the proposed equations give accurate predictions for the opening and closing moment capacity of the partially restrained apex brackets.

Table 2: Statistical results of the predicted moment capacities of apex brackets.

| Name | $R^2$ | *MAPE(%)* | *RMSE* | *AVE* | *STD* |
|---|---|---|---|---|---|
| $M_{o,tb}^{1a}$ | 0.99 | 5.17 | 1.68 | 1.00 | 0.07 |
| $M_{o,tb}^{2a}$ | 1.00 | 3.99 | 2.66 | 1.00 | 0.05 |
| $M_{c,tb}^{1a}$ | 0.97 | 6.06 | 3.79 | 1.01 | 0.08 |
| $M_{c,tb}^{2a}$ | 0.99 | 4.61 | 4.32 | 1.00 | 0.06 |

### 3.2 Eaves brackets with top-bottom stiffeners

The moment capacity of eaves brackets is further investigated by conducting a parametric study using the validated FE model shown in Figure 11, for the partially restrained eaves joints [15]. Six alternative cross-section geometries of the channels, identified by web size, are considered as tabulated in Table 3. The channels in the eaves joints are assumed to be linear elastic. The parameter of an eaves bracket is shown in Figure 12.

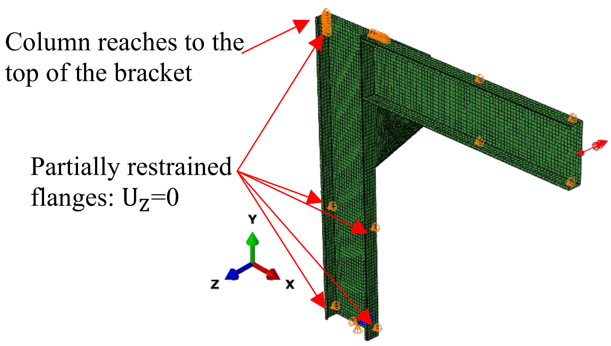


Figure 11: FE model for partially restrained eaves joint of 1B1C used in practice.

Table 3: Selected variable for parametric studies on eaves joints.

| Channel | $b_e$ (mm) | $b_e/a_e$ | $t$ (mm) | $f_y$ ($\mathrm{N/mm^2}$) | Unified geometric parametric |
|---|---|---|---|---|---|
| C150 | 150 | [0.4 ~ 0.9] | [2 ~ 4] | [250 ~ 550] | $\theta_a$ = 10º; $g_{cr}$ = 5 mm; $a_{eb}$= $b_{eb}$ = 40 mm; $d_s = 1.95a_t(t/a_t)^{0.543}$; Bolt distance ≤ 200 mm. |
| C200 | 200 | | | | |
| C250 | 250 | | | | |
| C300 | 300 | | | | |
| C350 | 350 | | | | |
| C400 | 400 | | | | |

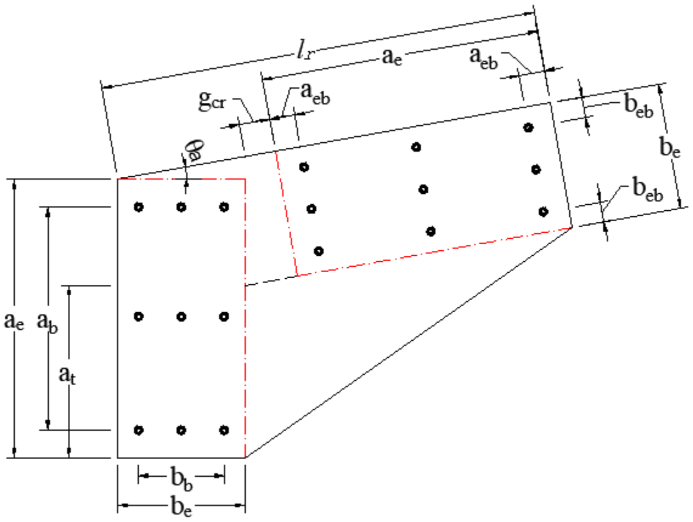


Figure 12: Diagram showing the parameter of an eaves bracket (dotted lines represent the outlines of channels).

### 3.2.1 Opening moment

In this study, a unified design equation for the moment capacity is created using a linear regression approach of machine learning. To predict the opening moment capacity of eaves brackets with top-bottom stiffeners, 2,520 FE models are employed.

The predicted opening moment capacity ($M_{o,tb}^{1e}$) of the single eaves bracket is shown in the following.

$$M_{o,tb}^{1e} = 4.1544\, a_e^{0.8741}\, b_e^{0.5352}\, f_y^{0.5929}\, t^{1.6176}\, 10^{-5} \tag{5}$$

Where, units of $a_e$, $b_e$, and $t$ is mm, the unit of $f_y$ is $\mathrm{N/mm^2}$, and the unit of $M_{o,tb}^{1e}$ is kN. m.

The opening moment ($M_{o,tb}^{2e}$) of back-to-back eaves brackets with top-bottom stiffeners can be calculated by the following equation:

$$M_{o,tb}^{2e} = 4.0847\, a_e^{1.1053}\, b_e^{0.3166}\, f_y^{0.7000}\, t^{1.6985}\, 10^{-5} \tag{6}$$

### 3.2.2 Closing moment

The 2,520 finite element models are utilized to anticipate the load-bearing capacity for the closing moment of eaves brackets. The closing moment capacity ($M_{c,tb}^{1e}$) of the single eaves bracket with top-bottom stiffeners can be predicted using the following equation:

$$M_{c,tb}^{1e} = 1.0117\, a_e^{0.9364}\, b_e^{0.3450}\, f_y^{0.4134}\, t^{1.9766}\, 10^{-4} \tag{7}$$

The closing moment ($M_{c,tb}^{2e}$) of back-to-back eaves brackets can be calculated by the following equation, based on the parametric study on 1,260 FE models of 2B2C.

$$M_{c,tb}^{2e} = 2.4022\, a_e^{1.2674}\, b_e^{-0.0503}\, f_y^{0.4401}\, t^{2.1270}\, 10^{-4} \tag{8}$$

Statistical results of the predicted moment capacities of eaves brackets are tabulated in Table 4. This outcome demonstrates that the proposed equations give accurate predictions for the opening and closing moment capacity of the partially restrained eaves brackets with top-bottom stiffeners.

Table 4: Statistical results of the predicted moment capacities of eaves brackets.

| Name | $R^2$ | *MAPE(%)* | *RMSE* | *AVE* | *STD* |
|---|---|---|---|---|---|
| $M^{1e}_{o,tb}$ | 0.98 | 5.44 | 3.28 | 1.00 | 0.08 |
| $M^{1e}_{c,tb}$ | 0.99 | 4.68 | 2.16 | 1.00 | 0.06 |
| $M^{2e}_{o,tb}$ | 0.99 | 5.48 | 6.56 | 1.00 | 0.07 |
| $M^{2e}_{c,tb}$ | 0.99 | 5.99 | 6.26 | 1.00 | 0.08 |

## 4 CONCLUSIONS

This study uses modelling techniques, validated against previously published experimental tests, to develop design equations for predicting the moment capacity of the partially restrained apex and eaves brackets. The ultimate load of the joints depends on the bracket strength when the channel has enough capacity to prevent buckling. The suggested geometrical parameters are presented for both apex and eaves brackets. Unified design equations are presented to calculate the moment capacity of the apex and eaves brackets commonly used in the construction of CFS portal frames, encompassing the opening and closing moments, considering both single and back-to-back brackets.

## NOTATIONS

| | |
|---|---|
| 1B2C | One bracket and two channels |
| 1B1C | One bracket and one channel |
| 2B2C | Two brackets and two channels |
| $a_a$ | Width of the triangular area of an apex bracket |
| $a_b$ | Length of bolt-group |
| $a_{ab}$ | The distance from the outline of the bolt group to the edge of an apex bracket |
| $a_e$ | Width of the triangular area of an eaves bracket |
| $a_{eb}$ | The distance from the outline of the bolt group to the edge of an eaves bracket |
| $a_t$ | The distance from the bottom of the eaves bracket to the extension of a rafter, shown in Figure 12 |
| $AVE$ | The mean value |
| $b_a$ | Edge width of the apex bracket |
| $b_b$ | Breadth of bolt-group |
| $b_{ab}$ | The distance from the outline of the bolt group to the edge of an apex bracket |
| $b_e$ | edge width of an eaves bracket |
| $b_{eb}$ | The distance from the outline of the bolt group to the edge of an eaves bracket |
| CFS | Cold-formed steel |
| $d_s$ | Depth of stiffener |
| EXP | Experimental |
| Eq. | Equation |
| $f_y$ | Yield stress |

| | |
|---|---|
| FEA | Finite element analysis |
| $g_r$ | The gap between rafters in an apex bracket |
| $g_{cr}$ | The gap between columns and rafters |
| $R^2$ | Coefficient of determination |
| $RMSE$ | Root-mean-square deviation |
| $MAPE$ | Mean-absolute-percentage error |
| $M_{o,tb}^{1a}$ | Equation prediction of opening moment capacity of a single apex bracket with top-bottom stiffeners |
| $M_{o,tb}^{2a}$ | Equation prediction of opening moment capacity of the back-to-back apex brackets with top-bottom stiffeners |
| $M_{c,tb}^{1a}$ | Equation prediction of closing moment capacity of a single apex bracket with top-bottom stiffeners |
| $M_{c,tb}^{2a}$ | Equation prediction of closing moment capacity of the back-to-back apex brackets with top-bottom stiffeners |
| $M_{o,tb}^{1e}$ | Equation prediction of opening moment capacity of a single eaves bracket with top-bottom stiffeners |
| $M_{o,tb}^{2e}$ | Equation prediction of opening moment capacity of the back-to-back eaves brackets with top-bottom stiffeners |
| $M_{c,tb}^{1e}$ | Equation prediction of closing moment capacity of a single eaves bracket with top-bottom stiffeners |
| $M_{c,tb}^{2e}$ | Equation prediction of closing moment capacity of the back-to-back eaves brackets with top-bottom stiffeners |
| $STD$ | Standard deviation |
| $t$ | Thickness |
| $\theta_a$ | The pitch of the portal frame |

## REFERENCES


[1] Lim, J. B. P., & Nethercot, D. A. (2002). Design and development of a general cold-formed steel portal framing system. *Structural Engineer*, 80(21), 31–40.

[2] Rinchen, R., & Rasmussen, K. J. (2020). Experiments on long-span cold-formed steel single C-section portal frames. *Journal of Structural Engineering*, 146(1), 04019187.

[3] Lim, J. B., & Nethercot, D. A. (2004). Stiffness prediction for bolted moment-connections between cold-formed steel members. *Journal of constructional steel research*, 60(1), 85-107.

[4] Australia/New Zealand Standard (AS/NZS). Cold-Formed Steel Structures, AS/NZS 4600:2018. *Standards Australia/ Standards New Zealand*; 2018.

[5] AISI (American Iron and Steel Institute) North American Specification for The Design of Cold-Formed Steel Structural Members. *AISI S100*. Washington, DC: AISI, 2016.

[6] EN 1993-1-3, Eurocode 3: Design of Steel Structures-Part 1-3: General Rules-Supplementary Rules for Cold-Formed Members and Sheeting, *European Committee for Standardization*, Brussels, Belgium, 2006.

[7] Lim, J. B. P., & Nethercot, D. A. (2002). F. E.-Assisted design of the eaves bracket of a cold-formed steel portal frame. *Steel & composite structures*, 2(6), 411-428.

[8] Chen, X., Blum, H. B., Roy, K., Pouladi, P., Uzzaman, A., & Lim, J. B. (2021). Cold-formed steel portal frame moment-resisting joints: Behaviour, capacity and design. *Journal of Constructional Steel Research*, 183, 106718.

[9] ABAQUS Inc. ABAQUS/CAE User's Guide, v6.14, Pawtucket, USA; 2014.

[10] Lim, J. B. P., Hancock, G. J., Charles Clifton, G., Pham, C. H., & Das, R. (2016). DSM for ultimate strength of bolted moment-connections between cold-formed steel channel members. *Journal of Constructional Steel Research*, 117, 196–203.

[11] Chen, X., Boston, M., Bell, D., Mares, J., Roy, K., & Lim, J. B. (2023). Moment capacity of apex brackets of cold-formed steel portal frames. *Thin-Walled Structures*, 185, 110574.

[12] Hu, S., Wang, W., & Lin, X. (2022). Two-stage machine learning framework for developing probabilistic strength prediction models of structural components: An application for RHS-CHS T-joint. *Engineering Structures*, 266, 114548.

[13] Tran, M. K., Panchal, S., Chauhan, V., Brahmbhatt, N., Mevawalla, A., Fraser, R., & Fowler, M. (2022). Python-based scikit-learn machine learning models for thermal and electrical performance prediction of high-capacity lithium-ion battery. *International Journal of Energy Research*, 46(2), 786-794.

[14] Tang, Z., Li, Z., & Wang, T. (2023). Probabilistic bearing capacity assessment for unequal-leg angle cross-bracings in transmission towers. *Journal of Constructional Steel Research*, 200, 107672.

[15] Chen, X., Boston, M., Bell, D., Roy, K., Mares, J., & Lim, J. B. (2023). Moment capacity of eaves brackets of cold-formed steel portal frames. *Thin-Walled Structures*, 189, 110947.